Fatigue experimental characterization of preloaded injection bolts in a metallic bridge strengthening scenario

Pedrosa, Bruno; Correia, José ; Rebelo, Carlos; Veljkovic, Milan; Gervásio, Helena

DOI
10.1016/j.engstruct.2021.112005

Publication date
2021

Document Version
Final published version

Published in
Engineering Structures

Engineering Structures 234 (2021) 112005

Contents lists available at ScienceDirect

Engineering Structures

journal homepage: www.elsevier.com/locate/engstruct

Fatigue experimental characterization of preloaded injection bolts in a metallic bridge strengthening scenario

Bruno Pedrosa [a,*], José Correia [b], Carlos Rebelo [c], Milan Veljkovic [d], Helena Gervásio [a]

[a] University of Coimbra, Institute for Sustainability and Innovation in Structural Engineering (ISISE), Department of Civil Engineering, 3030 – 790 Coimbra, Portugal
[b] CONSTRUCT & Faculty of Engineering, University of Porto, 4200-465 Porto, Portugal
[c] Institute for Sustainability and Innovation in Structural Engineering (ISISE), Department of Civil Engineering, University of Coimbra, 3030 – 790 Coimbra, Portugal
[d] Faculty of Civil Engineering and Geosciences, Delft University of Technology, Delft, Netherlands

ARTICLE INFO

Keywords:
Injection bolts
Fatigue
Old bridges
Structural strengthening
Shear connections

ABSTRACT

All over the world, the number of civil engineering structures, particularly bridges with long service periods, has been increasing. The most common evidences of damages are the presence of corroded metallic elements and cracks in structural details due to the fatigue phenomenon. A large number of cases were found in which fatigue cracks were detected in structural details, such as riveted connections. Different strategies can be implemented for repairing and strengthening operations of old metallic riveted bridges. However, the use of injection bolts has been considered as an alternative with important advantages. In this regard, it is essential to study their performance under fatigue loading. In this investigation, an experimental campaign has been performed to assess the fatigue strength of injection bolts by means of comparison with standard bolts. These fatigue tests are defined to be representative of a structural strengthening scenario of an old metallic bridge. Experimental results show that injection bolts contribute to significantly reduce the scatter in the data related to fatigue resistance. For double shear specimens, the characteristic curve proposed for connections with injection bolts presents a detail category with 15% higher value when compared to non-injected specimens. The beneficial effect is also verified in terms of slip deformation. For single shear specimens, the overall effect of the adhesive is not clear.

1. Introduction

Since the end of the 19th century, the number of metallic bridges constructed all over the world has been increasing. A significant number of these structures have long service lives and, therefore, they are prone to present high levels of structural degradation. For the majority, traffic intensity has increased significantly and their material properties have been degraded [1]. Scientific investigations have been showing that the most common evidences of structural damages in metallic bridges with long service lives are the presence of corroded elements and fatigue cracks [2–5].

There are several possibilities for repairing and strengthening operations on metallic riveted bridges, such as: implementation of fibre reinforced polymer (FRP) plates (bonded/unbonded and pre-stress/non pre-stressed) or addition of supplementary steel plates. FRP plates can be effective by restoring the capacity of a damaged steel section or even strengthen it for higher loads than originally designed. Recent studies have shown that fatigue strengthening of steel members with FRP composites is promising, namely by delaying initial cracking, reducing the crack growth rate, extend the fatigue life and decrease the stiffness decay with residual deflection [6–9]. Strengthening using additional steel plates can be conducted using rivets, welding, high strength friction grip bolts or injection bolts, however the use of injection bolts has been considered as a better solution concerning their mechanical performance and protection against corrosion [10,11]. Injection bolts can be used to connect new steel plates but also to replace faulty rivets.

Several authors [12–18] have investigated the fatigue strength behaviour of riveted, bolted and welded connections, as well as the characterization of its fatigue fracture mechanism. Hosseini et al. [12] presented an experimental characterization study of bolted shear connectors and local failure of concrete under static and fatigue loading conditions. Liu et al. [16] suggested a simplified fatigue approach based on the continuum damage mechanics for metallic bolted connections under uni- and multi-axial loading conditions. Leonetti et al. [14] proposed the fatigue life prediction of riveted shear connections based on a

* Corresponding author.
E-mail addresses: bruno.pedrosa@uc.pt (B. Pedrosa), jacorreia@fe.up.pt (J. Correia), crebelo@dec.uc.pt (C. Rebelo), M.Veljkovic@tudelft.nl (M. Veljkovic), hger@dec.uc.pt (H. Gervásio).

https://doi.org/10.1016/j.engstruct.2021.112005
Received 24 June 2020; Received in revised form 18 January 2021; Accepted 1 February 2021
Available online 2 March 2021
0141-0296/

Nomenclature

FRP	fiber reinforced polymer
ECCS	European Convention for Constructional Steelwork
A, B	linear regression parameters
A_s	tensile stress area of bolt
C	fatigue strength material constant
d	bolt diameter
f	frequency
$f(R_\sigma)$	normalization function to consider stress ratio effects
f_{ub}	ultimate strength of bolt
$F_{net,Rd}$	analytical tensile resistance
$F_{p,C}$	applied preload on bolt
F_s	experimental slip resistance
F_u	experimental ultimate resistance
k	correlation coefficient for bolt preload
$k_{(1-\alpha_n),p_n,n}$	one-sided tolerance limit for a normal distribution
m	inverse slope of fatigue strength curve
M	applied torque on bolt
n	sample size
N_f	number of cycles at failure
p_n	probability of failure
q	parameter to distinguish between unknown value of inverse slope or fixed value
R^2	coefficient of determination
R_σ	stress ratio
s	standard deviation
X	independent variable
X_j	value of the independent variable for tested specimen j
$\overline{X}$	mean value ofX_j
Y	dependent variable
Y_j	value of the dependent variable for tested specimen j
$\overline{Y}$	mean value ofY_j
α_n	parameter to define confidence level
$\Delta\sigma$	stress range
$\Delta\sigma_{gross}$	stress range at gross cross-section
$\Delta\sigma_{gross,norm}$	normalized stress range at gross cross-section
$\Delta\sigma_{norm}$	normalized stress range

reliability modelling combined with local approaches.

Injection bolts can be produced from standard bolts adapting them for the injection process [19]. As is shown in Fig. 1, the gap between the plates and the bolt shank is filled with an adhesive. After the curing process, it is intended to obtain a slip resistant connection. Most of the studies focused on the static or quasi-static performance of injection bolts [20–22] showing that this methodology has good results.

Recent investigations have been made in order to evaluate the potential of different materials to be used in the injection. Rodrigues et al. [23] made an experimental characterization of two structural adhesives aiming to obtain their performance under static and fatigue loading conditions. Results showed that the epoxy-based resin Sikadur®-52 is suitable to be used in injection bolts. Koper [24] studied the application of epoxy-based resins on injection bolts under static loading, concluding that the viscosity is the first parameter to be accounted for in order to achieve a successful injection. Low values of viscosity are not adequate because the adhesive easily gets out of the cavity, and high values of viscosity make the injection process very difficult and it is not easy to guarantee that all the space is filled up. Kolstein et al. [25] also found that grout materials, such as Sikadur®-30, are not adequate for injection bolts. In Nijgh [26], an innovative solution was created by filling the space with steel shots prior to injection with resin. This reinforced resin was created to increase connection stiffness and improve its creep performance. Additionally, experimental, numerical, and analytical assessments of compressive behaviour under confined and unconfined conditions for different adhesives to be used in injection bolts were studied by different authors [27,28]. It was found that steel-reinforced resin has higher compressive strength values and shows to be a promising solution for injection bolts.

The application of preload on bolted connections influences the fatigue behaviour, mainly because the load transfer mechanism is by friction of plates when preload forces are implemented, and by shear of bolts and bearing of plates when there is no preload. For bolted connections designed as bearing-type, fatigue crack initiates at the edge of the hole and grows in the region of the net cross-section. This is typical for bolted connections where the applied load exceeds the slip resistance of faying surfaces [29]. In the case of preloaded bolted connections, stress concentration occurs in the geometric discontinuity between outer and inner plates and between washers and outer plates. This type of fatigue failure is governed by the fretting corrosion mechanism and is obtained at the gross cross-section of plates [30,31]. The influence of preload magnitude on the fatigue life of bolted connections was assessed by Jiménez-Peña et al. [31] by means of experimental and numerical investigations. Results showed that higher fatigue performance can be obtained with higher preload forces. In fact, the beneficial effect of preload has been proven by several authors [32–35].

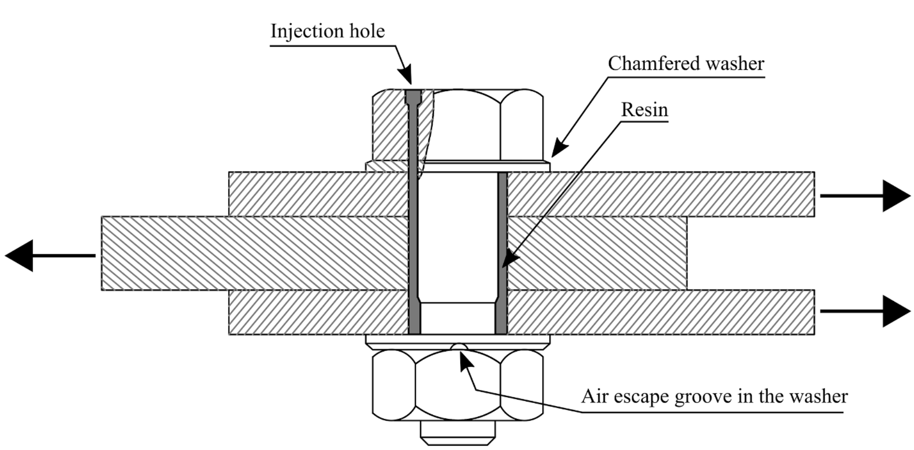

Fig. 1. Injection bolt configuration.

For single shear connections, there is one fundamental aspect related to the eccentricity in the neutral line. The main differences between connections with and without eccentricities are additional tensile load (which causes bending on the plates) and asymmetric loading conditions in the fastener leading to an inhomogeneous bearing pressure along the hole [36].

In what concerns fatigue design recommendations, the following S-N curves are proposed in EC3-1-9 (2005) [37]: detail category 112 should be used for double-covered symmetrical joints with preloaded high strength bolts or preloaded injection bolts; detail category 90 should be used for double-covered joints with fitted bolts or non-preloaded injection bolts, and one-sided connections with preloaded high strength bolts or preloaded injection bolts. Additionally, in 1994, the European Convention for Constructional Steelwork (ECCS) published a document called *European Recommendations for Bolted Connections with Injection Bolts* [10] with practical guidelines for static and fatigue design. However, the fatigue strength characterization of bolted connections with injected bolts combining puddle iron plates and current structural steels plates is not yet studied. The structural reinforcement of existing metallic bridges is frequently done considering the replacement of old metallic elements by structural elements of current steel [38]. Wang et al. [39] presented a fatigue performance study on ancient metallic bridges using reinforcement techniques based on the application of new steel plates through bonding or bolting. In this sense, the fatigue strength characterization and the identification of failure mechanisms of structural connections combining existing metallic plates and current steel plates deserves special attention, especially the definition of reliable S-N curves.

In this paper, an experimental campaign is addressed in which fatigue tests have been conducted on preloaded bolted connections with injected and non-injected bolts aiming to understand the influence of the adhesive and to define reliable S-N design curves. Specimens were built combining current and old material plates. Additionally, results are compared with the design S-N curves included in EC3-1-9 [37] and proposed by Taras and Grainer [40]. It should be stated that the comparison between structural components composed with old metallic materials and current standards has been done by DiBattista et al. [41].

2. Experimental campaign

A total of 45 specimens have been tested varying the type of connection (single and double shear), type of bolt (injected and non-injected) and stress range (high, medium and low). The geometry of specimens is presented in Fig. 2.

Single shear connections are composed of one S355 steel plate and one puddle iron plate, while double shear connections are composed of two puddle iron plates positioned on the same side and one S355 steel plate in the opposite side. Puddled iron plates were extracted from the web of the main girders of a centenary Portuguese bridge named Eiffel bridge – see Fig. 3. It was inaugurated in 1886 and was built in puddled iron, which is a material with many heterogeneities responsible for significant scatter in its properties [42]. Holes in plates were then executed in a set of steps: drills were used first for spotting and then for complete drilling; then helical boring was implemented to enlarge the holes to its required size; and finally, surfaces of the hole were finished with a boring head. This execution of holing reduces the presence of geometrical defects which could influence negatively the fatigue life.

High strength bolts (class 10.9) were used in the assembly, and preload forces were applied using the torque method and the procedure described in EN 1090-2 [19]. The specified bolt preload is obtained by $F_{p,C} = 0.7 \cdot f_{ub} \cdot A_s = 247\ kN$, where f_{ub} is the ultimate tensile strength of the bolt and A_s is the tensile stress area. Furthermore, the correlation between the torque, M, and the specified preload force, $F_{p,C}$, is given by $M = k \cdot d \cdot F_{p,C} = 729\ N.m$, where k is the correlation coefficient (0.123) and d is the bolt diameter.

Corrosion was removed from the plate contact surfaces. However, it was intended to obtain reduced load transfer by friction in order to achieve fatigue failure at net cross-section of plates because, with this failure pattern, the influence of the adhesive placed around the bolt shank is more effective comparing the case of fatigue failure at gross cross-section of plates. The adhesive used for injection bolts was the epoxy-based resin Sikadur®-52. It is a two-part epoxy resin with low viscosity and good adhesion to steel. The mechanical properties with 7 days of curing and 23 °C presented by the manufacturer are the following: compressive strength – 34 MPa; tensile strength – 24 MPa. The pot life of Sikadur®-52 is 25 min at 20 °C, approximately [44]. Specimens with resin-injected bolts were subjected to a cure time of at least 7 days, which resulted into near maximum strength properties.

Fig. 3. Eiffel bridge – Viana do Castelo, Portugal [43].

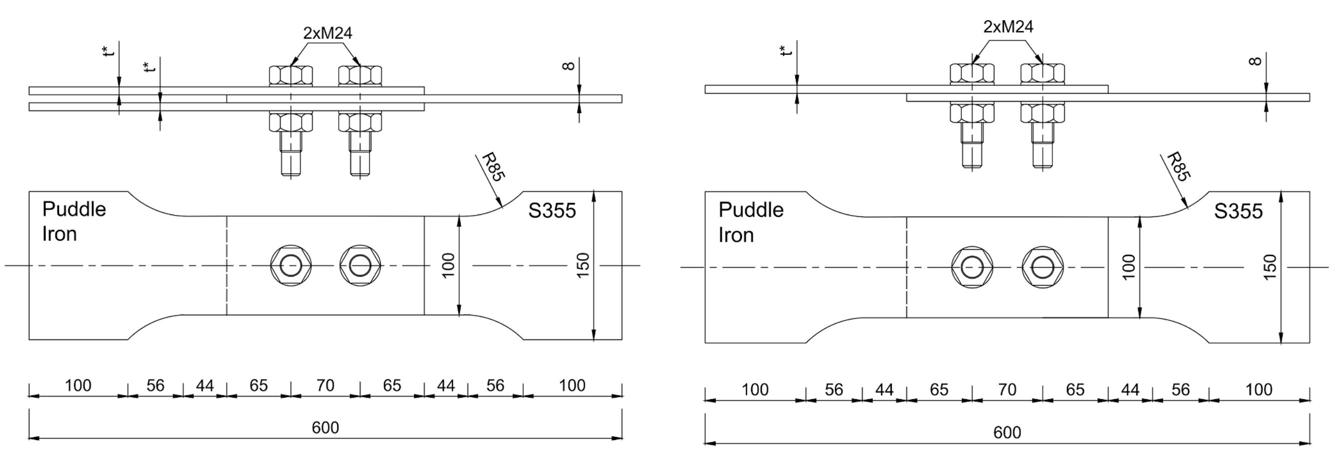

Fig. 2. Geometry of specimens (*thickness varies between 6 and 8 mm): a) single shear; b) double shear. (dimensions in mm).

3. Statistical analysis and stress ratio normalization

According to ISO 12107 [45] and EC3-1-9 [37], fatigue experimental data is represented with the applied stress range, $\Delta\sigma$, and number of cycles, N_f, using a logarithmic scale. This methodology allows to define a linear expression (Basquin model) between those parameters as is described in the following equation:

$$\log N_f = \log C + m\cdot\log\Delta\sigma \tag{1}$$

where m is the inverse slope and $\log C$ is the intersection with the axis $\log\Delta\sigma$.

Thereby, a mean S-N curve can be defined for the obtained results using a linear regression analysis based on the least squares method. In this sense, variables of linear expression presented in Eq. (2) are defined as: dependent variable Y, defined as $Y = \log N_f$; independent variable X, as $X = \log\Delta\sigma$; B is computed using Eq. (3), where $\overline{Y}$ and $\overline{X}$ are the mean values of the experimental data $X_j = logN_j$ and $Y_j = log\Delta\sigma_j$, respectively, and n is the sample size:

$$Y = A + B\cdot X \tag{2}$$

$$B = \frac{\sum_{j=1}^{n}(X_j - \overline{X})(Y_j - \overline{Y})}{\sum_{j=1}^{n}(X_j - \overline{X})^2} \tag{3}$$

$$A = \overline{Y} - B\cdot\overline{X} \tag{4}$$

Moreover, a characteristic S-N curve can be established as the lower limit corresponding to a probability of failure, p_n, for the population at a confidence level $(1-\alpha_n)$ and for a sample size n using the following equation:

$$\log N_f = \log C + m\cdot\log\Delta\sigma - k_{(1-\alpha_n),p_n,n}\cdot s \tag{5}$$

where $k_{(1-\alpha_n),p_n,n}$ is the one-sided tolerance limit (computed in the software MATLAB® using functions developed by Viktor Witkovsky [46]) for a normal distribution which depends on the confidence level, $(1-\alpha_n)$, probability of failure, p_n, and sample size, n. The last parameter s is the standard deviation computed with Eq. (6), where q is equal to 2 for analysis with no fixed value for the inverse slope of the S-N curve, and equal to 1 for analysis with a fixed value for the inverse slope [47]:

$$s^2 = \frac{\sum_{j=1}^{n}(Y_j - A - B\cdot X_j)^2}{n-q} \tag{6}$$

A characteristic S-N curve can be established using the requirements prescribed in EN 1993-1-9 [37] which are: 75% confidence level and 5% probability of $\log N_j$ to be exceeded for a normal distribution. Furthermore, it is also necessary to consider mean stress effects. Thus, experimental data used in this paper were normalized by computing the normalized stress range, $\Delta\sigma_{norm}$, as is shown in Eq. (7), this methodology being proposed by Taras and Greiner [40]:

$$\Delta\sigma_{norm} = \frac{\Delta\sigma}{f(R_\sigma)} \tag{7}$$

where $\Delta\sigma$ is the stress range applied during the experimental test and $f(R_\sigma)$ is a normalization function to consider stress ratio effects. This function depends on the year when the bridge was built. For wrought iron and mild steel manufactured before 1900, $f(R_\sigma)$ is defined as:

$$f(R_\sigma) = \begin{cases} \dfrac{1-R_\sigma}{1-0.7\cdot R_\sigma}, & if \ -1 \le R_\sigma \le 0 \\ \dfrac{1-R_\sigma}{1-0.75\cdot R_\sigma}, & if \ R_\sigma > 0 \end{cases} \tag{8}$$

For mild steel after 1900 (S235, S275 and S355), the following normalization function is proposed:

$$f(R_\sigma) = \begin{cases} \dfrac{1-R_\sigma}{1-0.4\cdot R_\sigma}, & if \ -1 \le R_\sigma \le 0 \\ \dfrac{1-R_\sigma}{1-0.6\cdot R_\sigma}, & if \ R_\sigma > 0 \end{cases} \tag{9}$$

4. Experimental tests – Single shear specimens

4.1. Preliminary static test

A single shear specimen with the geometry presented in Fig. 2a) has been tested under monotonic loading conditions. Normal bolts are used (without resin) and all the conditions related to preload force and surface treatment are the same as those used in fatigue tests. This test has been conducted under displacement control (0.01 mm/s). The force-displacement curve of this monotonic test is plotted in Fig. 4. The failure mode occurs at the net cross-section of the puddle iron plate.

The analytical tension resistance, $F_{net,Rd}$, computed with Equation 6.8 of EC3-1-1 [48] is 147.3 kN. The slip resistance is obtained from the test as $F_s = 64$ kN and the ultimate resistance as $F_u = 180.8$ kN. Taking into account the obtained values, fatigue tests have been defined considering that the maximum load should be superior to the slip resistance of the connection in order to obtain load transfer by bearing of the resin and inferior to the analytical tension resistance.

4.2. Fatigue tests

Specimens have been tested on a WALTERBAI Testing Machine rated to 600 kN (Fig. 5). All fatigue tests have been carried out under load control with a stress R-ratio equal to 0.1. Test frequency is set to 5 Hz for all tests except for high-cycle fatigue tests where test frequency is defined as 10 Hz. The presence of the adhesive requires low values of frequency. ASTM D7791 [49] indicates a test frequency between 1 and 25 Hz and recommends the lowest value as much as possible. When no fatigue failure is obtained at 5 million cycles, the test is stopped, and is considered as a run-out. This value corresponds to the constant amplitude fatigue limit defined in EC3-1-9 [37]. Experimental results of fatigue tests on single shear specimens are presented in Table 1. Failures occurred in the puddle iron plate for all specimens, except for specimen No. 10 (rupture in S355 plate) due to adhesive partial injection. Some non-valid data was found due to deficient injection of the resin or early rupture.

It was found a correlation between the applied stress range and the location of fatigue failure. Higher values of applied stress range mainly conducted to failure pattern through the net cross-section of plates while lower values of applied stress range mainly conducted to failure pattern through the gross cross-section of plates. Fig. 6 presents pictures from gross and net failures, injection bolts, and fracture surface on puddle iron plate.

The use of injection bolts should contribute to increase the stiffness of the connection and the slip displacement during fatigue tests should be lower when compared to standard bolted connections. Maximum deformation was recorded in every cycle during fatigue tests aiming to analyse the influence of the adhesive, therefore, in Fig. 7 is shown the evolution of slip displacement for two fatigue tests (standard vs injected) for each stress level ($\Delta\sigma_1$ to $\Delta\sigma_4$). It is observed that using injected bolts contributed to decrease the slip of the connection. Taking into account only the tests presented in Fig. 7, the reduction is around 60%.

Experimental fatigue data is presented in the S-N diagram in Fig. 8. Stress range values are computed using gross cross-section area of puddle iron plate, as is recommended in EC3-1-9 [37] for preloaded bolted connections, and Eq. (8) is used for normalization regarding the influence of the stress ratio. Then, the statistical analysis described in Section 3 is applied. The mean S-N curve for standard bolted connections is characterized by an inverse slope of $m = 5.1$, whereas the mean S-N curve for bolted connections with injection bolts has an inverse slope of

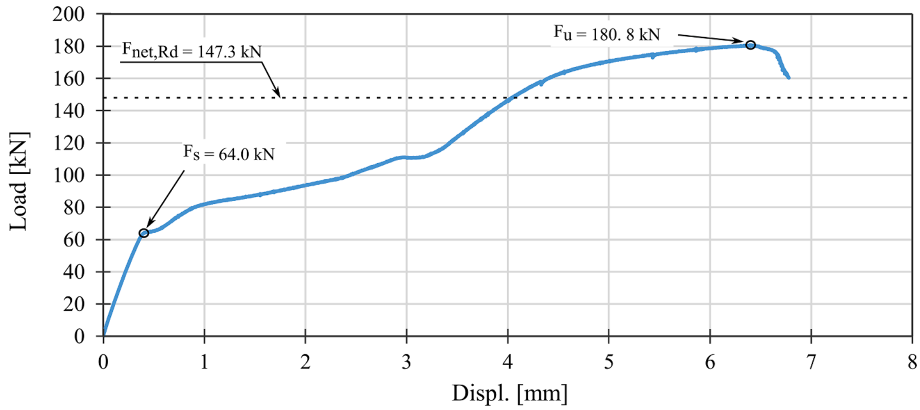

Fig. 4. Monotonic test on single shear connection.

Fig. 5. Fatigue test on single shear bolted connection.

$m = 6.9$. The level of scatter can be assessed by the coefficient of determination (R^2). It is observed that implementing injection bolts contribute to reduce the level of scatter, since fatigue data for standard bolts has $R^2 = 0.5$ while fatigue data for injection bolts has $R^2 = 0.8$. In order to determine mean S-N curves whose inverse slope values are natural numbers, new statistical analysis has been performed, in this case, imposing that the value of the inverse slope is the closest natural value to 6.9 in the case of injection bolts (which is 7) and to 5.1 in the case of standard bolts (which is 5).

Table 2 shows a comparison of fatigue life (computed on characteristic curves from Fig. 8) for preloaded injection bolts and preloaded standard bolts on each stress range separately. It can be observed that the beneficial effect on the fatigue strength by using preloaded injection bolts is evident in all stress levels but with higher relevance for high-cycle fatigue regimes. The fundamental aspect is that the lower level of scatter verified for data from preloaded injection bolts led to higher fatigue strength in the characteristic curve for all fatigue regimes. In fact, on average, using preloaded injection bolts leads to 8.6% higher fatigue lives for the studied stress ranges.

However, due to the high level of scatter, the difference in the value of the inverse slope (7 for injection bolts and 5 for standard bolts) and the low quantity of data, authors decided to propose a S-N curve for all data from single shear specimens as is shown in Fig. 9. It was found that the optimal mean S-N curve has an inverse slope (m) with a value of 6.3 and a coefficient of determination (R^2) with a value of 0.7. In order to determine a mean S-N curve whose inverse slope value is a natural number, a new mean S-N curve has been defined, in this case imposing that the value of the inverse slope is the closest natural value of 6.3 (which is 6). In this sense, in the following analysis, only the curve with an inverse slope equal to 6 is used.

In Fig. 10, fatigue experimental data from single shear bolted connections is compared to the design recommendation on EC3-1-9 [37]. Note that the detail category recommended in this standard (detail category 90) does not represent a safe design criterion. In fact, this design curve is not able to represent the fatigue strength of old metallic materials, as was already discussed by several authors [42,50]. Taras and Greiner [40] performed an analysis of a significant amount of fatigue tests using riveted connections from old bridges. They proposed a design S-N curve with an inverse slope $m = 5$ and a detail category of 71 for single shear riveted connections. This curve seems to be adequate to represent fatigue experimental data obtained in this experimental campaign.

5. Experimental tests – Double shear specimens

5.1. Preliminary static test

The procedure implemented for single shear specimens has also been used for double shear specimens. In this sense, the first step was to perform a static test in order to define all the parameters for cyclic tests. Load and displacement values were recorded throughout the test, resulting in the curve shown in Fig. 11. The failure mode occurred at the net cross-section of S355 plate. It was verified that the slip resistance is $F_s = 104$ kN. The design tension resistance $F_{net,Rd}$ computed with Equation 6.8 of EC3-1-1 [48] is obtained as 210.2 kN. It is used as the upper limit of the load used in fatigue tests, while the slip resistance is used as a lower limit.

Table 1
Fatigue experimental results from single shear bolted connections.

Stress level	Specimen	Resin Injected	$\Delta\sigma_{gross}$ [MPa]	$\Delta\sigma_{gross,norm.}$ [MPa]	f [Hz]	N_f [cycles]	Obs.
$\Delta\sigma_1$-low cycle	1		180	175	5	5 678	Invalid
	2		166	161	5	164 054	Gross c. s. failure
	3		172	168	5	40 220	Net c. s. failure
	4	x	177	173	5	21 135	Net c. s. failure
	5	x	172	168	5	132 357	Mean c. s. failure
$\Delta\sigma_2$-medium cycle	6		159	154	5	325 628	Net c. s. failure
	7		153	149	5	57 990	Invalid
	8		157	153	5	29 028	Invalid
	9	x	156	152	5	175 045	Gross c. s. failure
	10	x	137	133	5	277 647	Invalid
	11	x	157	153	5	349 915	Gross c. s. failure
$\Delta\sigma_3$-medium cycle	12		129	126	5	50 725	Invalid
	13		131	127	5	675 759	Gross c. s. failure
	14		133	130	5	92 855	Net c. s. failure
	15	x	136	132	5	574 138	Net c. s. failure
	16	x	133	129	5	531 952	Mean c. s. failure
	17	x	129	126	5	413 977	Net c. s. failure
$\Delta\sigma_4$-high cycle	18		111	108	5	5 087 414	Run-out
	19		121	118	5	601 553	Mean c. s. failure
	20		117	114	5	905 699	Mean c. s. failure
	21	x	115	112	5	703 018	Gross c. s. failure
	22	x	116	113	5	1 289 745	Gross c. s. failure
	23	x	119	115	5	1 667 047	Gross c. s. failure
	24	x	111	108	10	5 115 822	Run-out

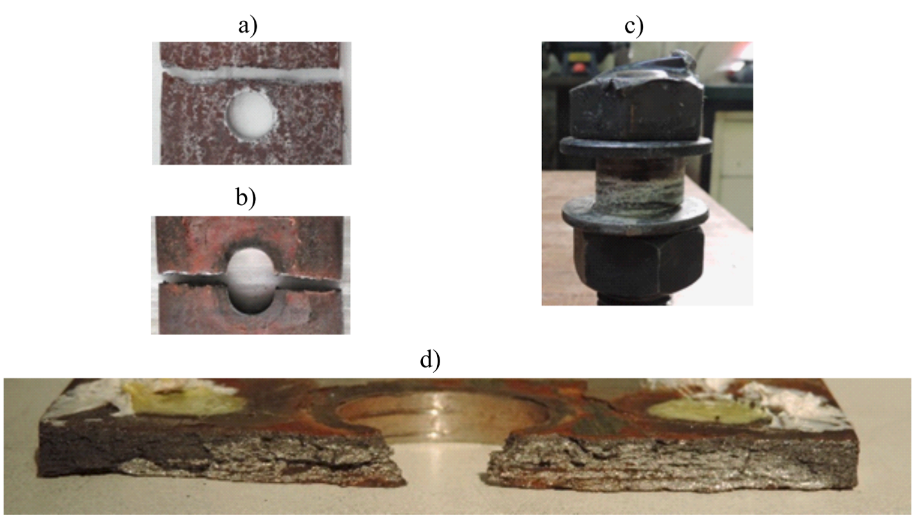

Fig. 6. Analysis of single shear specimens after fatigue test.

5.2. Fatigue tests

Fatigue tests on double shear specimens have been conducted using the same conditions of fatigue tests on single shear specimens, namely in what concerns: testing machine, stress ratio, frequency and stop criterion. The only exception was the frequency of test with specimen No. 22 which was set to 4 Hz. Fatigue experimental data is presented in Table 3. Failure mode is obtained at the S355 plate for the majority of the tested specimens.

In what concerns slip displacement of double shear specimens during fatigue tests, in Fig. 12 is shown the evolution of slip for two fatigue tests (standard vs injected) for each stress level ($\Delta\sigma_1$ to $\Delta\sigma_4$). For the selected fatigue tests, slip displacement for standard specimens is above 3 mm while for injected specimens it is below 1.5 mm. The increase of stiffness (slip reduction) in this case is higher when compared to single shear specimens (around 80% in this case), which means that the beneficial effect of using injection bolts is superior for double shear configuration.

The statistical analysis described in Section 3 is implemented on fatigue data from double shear specimens. The stress range is computed in the gross cross-section of the S355 steel plate and the influence of the stress ratio was considered by applying Eq. (9). The mean S-N curve for standard bolted connections is characterized by an inverse slope of $m = 6.7$, whereas the mean S-N curve for bolted connections with injection bolts has an inverse slope of $m = 7.0$. Note that implementing injection bolts contribute to reduce the level of scatter, since fatigue data for standard bolts have $R^2 = 0.5$ while fatigue data for injection bolts have $R^2 = 0.9$. New analytical analysis is then implemented using 7 as the inverse slope of S-N curves from specimens with standard and injection bolts and the results are shown in Fig. 13.

The fatigue strength improvement produced by preloaded injection bolts is materialized in an increase of 25 MPa in the characteristic S-N curve ($\Delta\sigma_{C,Injection} = 186$ MPa and $\Delta\sigma_{C,Standard} = 161$ MPa). The comparison of fatigue life (computed on characteristic curves) between preloaded injection bolts and preloaded standard bolts can be made for each stress range separately as is presented in Table 4. It can be observed that the effect on fatigue strength by using preloaded injection bolts is

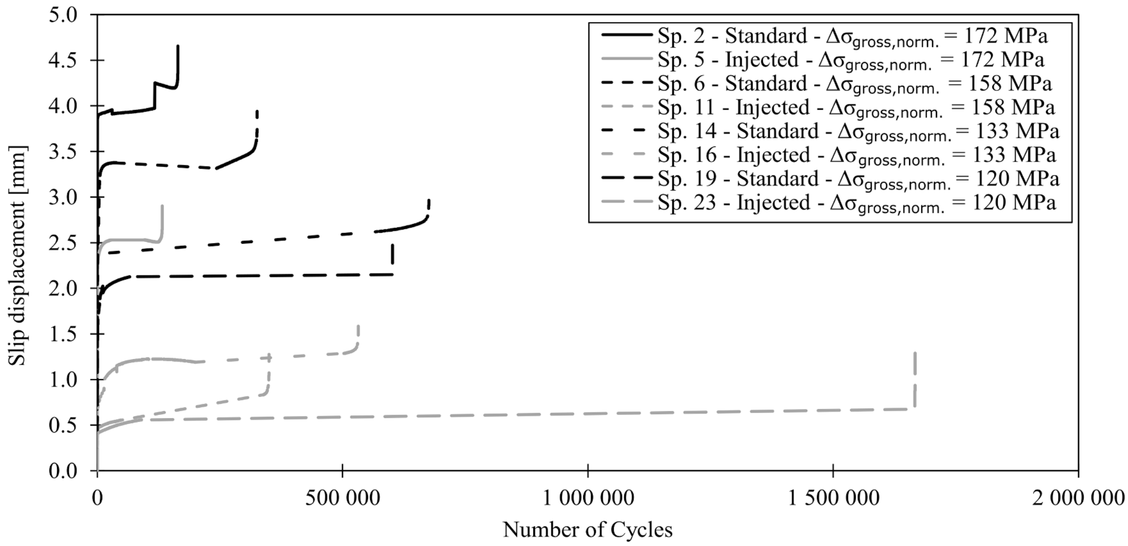

Fig. 7. Slip displacement during fatigue tests – single shear specimens.

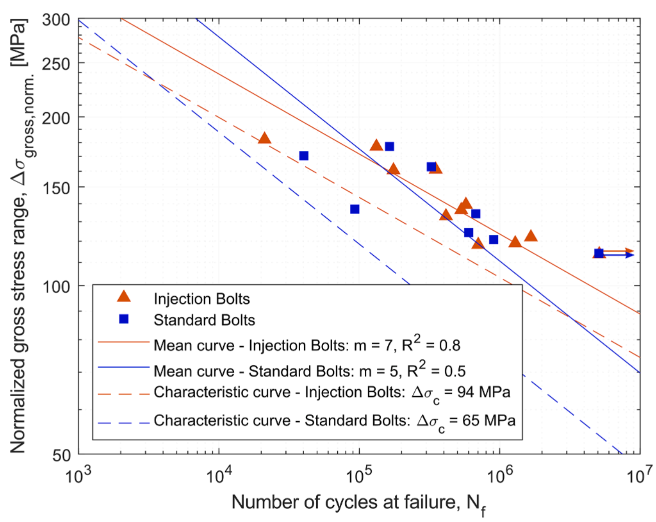

Fig. 8. Experimental data for single shear specimens (injection vs. standard bolts): mean and characteristic curves with fixed slope.

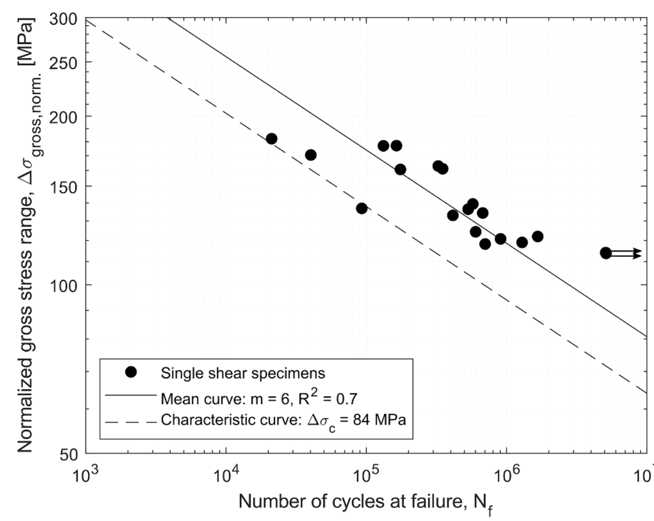

Fig. 9. Experimental data for single shear specimens (all data): mean and characteristic curves with fixed inverse slope.

Table 2
Comparison of fatigue life from preloaded standard and injection bolts for each stress range in the obtained characteristic curves – single shear specimens.

Stress range	Bolt type	Number of cycles N_f	Comparison (logarithmic values)
$\Delta\sigma_1 = 178$ MPa	Standard	13 089	
	Injection	22 252	+5.6%
$\Delta\sigma_2 = 162$ MPa	Standard	20 961	
	Injection	43 024	+7.2%
$\Delta\sigma_3 = 136$ MPa	Standard	50 269	
	Injection	146 400	+9.9%
$\Delta\sigma_4 = 119$ MPa	Standard	98 008	
	Injection	372 807	+11.6%

beneficial for all stress ranges. Furthermore, it is verified that the average value of the beneficial effect by using injection bolts is 8.4%.

In Fig. 14, fatigue experimental data from double shear bolted connections is compared to the design recommendation on EC3-1-9 [37]. It is remarked that only one data points (from standard bolts) stand below

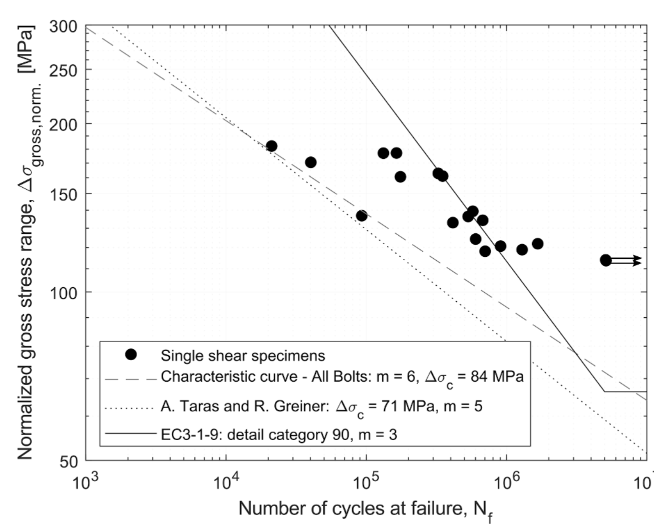

Fig. 10. Experimental data from single shear specimens: design curves.

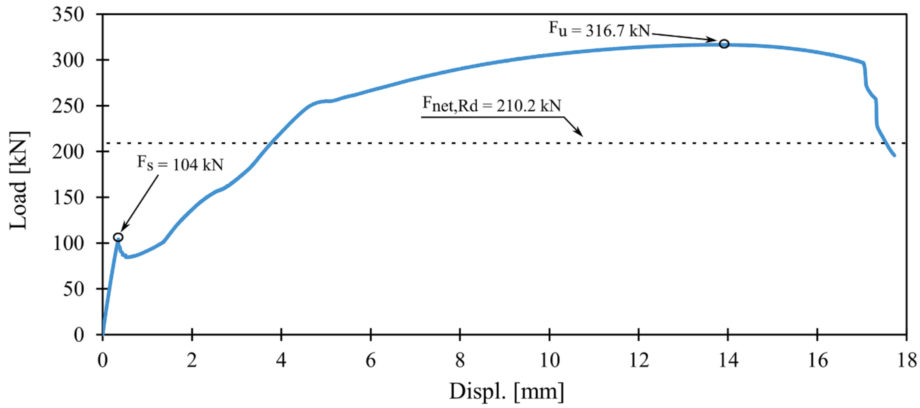

Fig. 11. Monotonic test of double shear specimen.

Table 3
Fatigue experimental results from double shear bolted connections.

$\Delta\sigma$	Specimen	Resin	$\Delta\sigma_{gross}$ [MPa]	$\Delta\sigma_{gross,norm}$ [MPa]	f [Hz]	N_f [cycles]	Obs.
$\Delta\sigma_1$ (low cycle)	1		250	261	5	440 260	Net c. s. failure
	2		250	261	5	648 250	Mean c. s. failure
	3		250	261	5	91 024	Net c. s. failure
	4	x	250	261	5	340 283	Net c. s. failure
	5	x	250	261	5	510 796	Net c. s. failure
	6	x	250	261	5	314 980	Net c. s. failure
$\Delta\sigma_2$ (medium cycle)	7		222	232	5	250 165	Net c. s. failure
	8		222	232	5	892 015	Mean c. s. failure
	9		222	232	5	1 596 924	Net c. s. failure
	10	x	222	232	5	1 118 960	Mean c. s. failure
	11	x	222	232	5	791 521	Net c. s. failure
	12	x	222	232	5	856 283	Mean c. s. failure
$\Delta\sigma_3$ (medium cycle)	13		197	206	5	1 088 528	Mean c. s. failure
	14		198	207	5	1 606 433	Net c. s. failure
	15		197	206	5	1 471 636	Mean c. s. failure
	16	x	198	206	5	5 000 000	Run-out
	17	x	197	206	5	5 000 000	Run-out
	18	x	197	206	5	1 128 094	Mean c. s. failure
$\Delta\sigma_4$ (high cycle)	19		175	183	10	5 000 000	Run-out
	20		186	195	10	2 292 737	Gross c. s. failure
	21		187	195	10	5 000 000	Run-out
	22	x	187	195	4	4 234 000	Gross c. s. failure

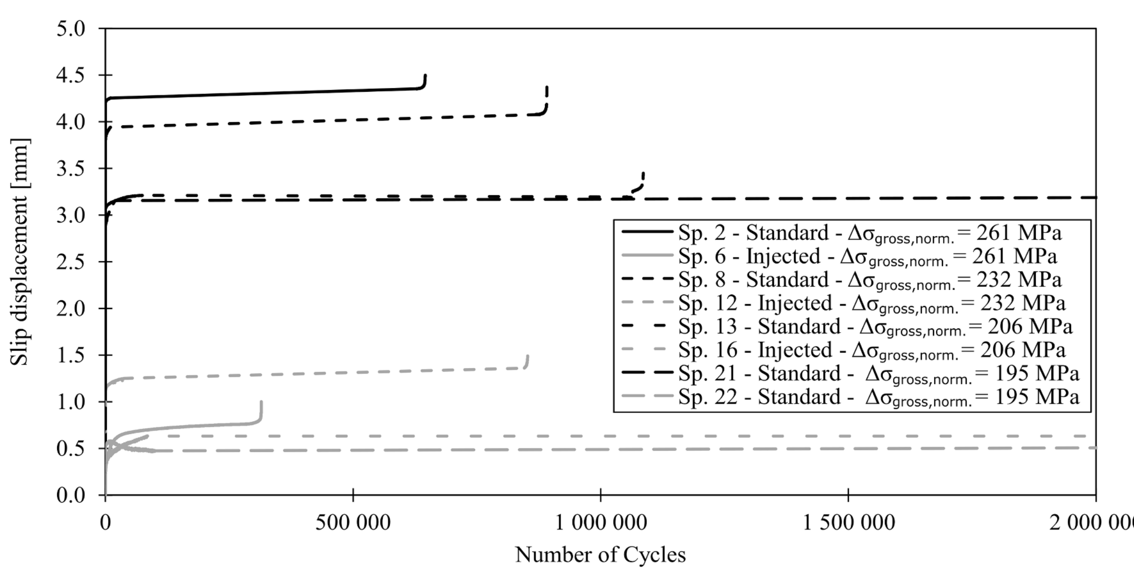

Fig. 12. Slip displacement during fatigue tests – double shear specimens.

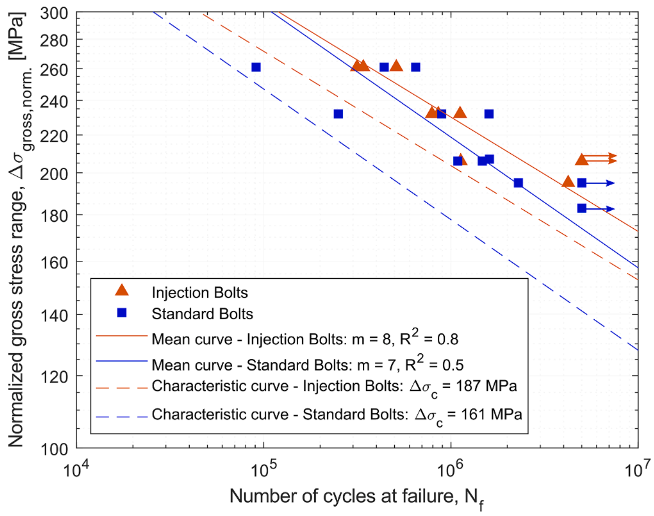

Fig. 13. Experimental data for double shear specimens (injection vs. standard bolts): mean and characteristic curves with fixed inverse slope.

Table 4
Comparison of fatigue life from preloaded standard and injection bolts for each stress range in the obtained characteristic curves – double shear specimens.

Stress range	Bolt type	Number of cycles N_f	Comparison (logarithmic values)
$\Delta\sigma_1 = 261$ MPa	Standard	67 931	
	Injection	188 298	+9.2%
$\Delta\sigma_2 = 232$ MPa	Standard	154 930	
	Injection	429 451	+8.5%
$\Delta\sigma_3 = 206$ MPa	Standard	356 025	
	Injection	986 868	+8.0%
$\Delta\sigma_4 = 195$ MPa	Standard	522 767	
	Injection	1 449 063	+7.7%

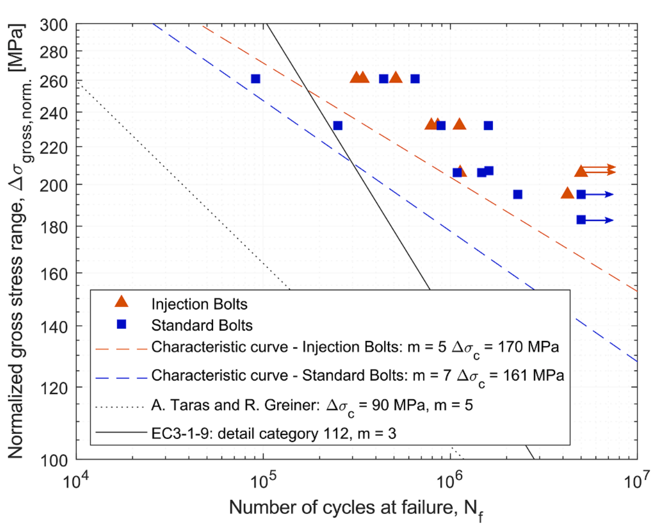

Fig. 14. Experimental data from double shear specimens: design curves.

the suggested curve. Taras and Greiner [40] proposed a design S-N curve with an inverse slope, $m = 5$, and fatigue strength of 90 MPa at 2 million cycles for double shear riveted connections. It represents a very conservative design criterion and is not adequate for this detail.

6. Conclusions

Preloaded bolted connections have been tested under fatigue loading conditions to compare the performance of standard bolts to injection bolts.

It is found that using preloaded injection bolts instead of preloaded standard bolts on single lap connections contributes to increase the stiffness by reducing the slip displacement in around 60%. Fatigue data was analysed using a statistical methodology which showed a significant level of scatter. Mean and characteristic S-N curve were defined and the value for the inverse slope obtained for preloaded injection bolts and preloaded standard bolts was distinct. Even if the comparison of fatigue life computed on characteristic curves presented an average increase of 8.6% when preloaded injection bolts, the high level of scatter, the difference in the value of the inverse slope and the low quantity of data led the authors to propose a unique characteristic curve computed using all data from single shear specimens. Since fatigue failure is obtained in puddle iron plates, experimental data is better correlated with the design curve proposed by Taras and Greiner than with the design curve proposed in Eurocode 3.

For double shear specimens, the reduction on slip displacement by using preloaded injection bolts is superior than for single shear specimens. On this detail, the resin around the bolt shank is more effective and the reduction of slip displacement is around 80%. Fatigue failure mainly occurs at the net cross-section, and the beneficial effect of the adhesive is visible and consistent. The statistical analysis shows that experimental data for both preloaded injection bolts and preloaded standard bolts can be represented by a S-N curve with an inverse slope of 7 and it enables to verify that using preloaded injection bolts leads to a characteristic curve with a detail category 15% higher. Since fatigue failure is obtained mainly at the S355 steel plate, fatigue strength results are not distant from those represented by the design curve proposed in Eurocode 3. On the other hand, the design recommendation made by Taras and Greiner is not adequate for the studied detail.

There is one additional benefit from implementing injection bolts verified on both single and double specimens. This benefit is related to the reduction of scatter on the results. Lower values of scatter are important in order to allow the determination of reliable design criteria. Present results show that for high-cycle fatigue regimes there is a significant beneficial effect of using injection bolts. Furthermore, future experimental investigations should focus on using only plates with current metallic materials and injection bolts with various high-performance adhesives.

CRediT authorship contribution statement

Bruno Pedrosa: Conceptualization, Methodology, Validation, Formal analysis, Investigation, Writing - original draft, Visualization. **José Correia:** Conceptualization, Methodology, Validation, Resources, Writing - review & editing, Visualization, Supervision, Project administration. **Carlos Rebelo:** Conceptualization, Methodology, Validation, Resources, Writing - review & editing, Visualization, Supervision, Project administration, Funding acquisition. **Milan Veljkovic:** Supervision. **Helena Gervásio:** Supervision, Funding acquisition.

Declaration of Competing Interest

The authors declare that they have no known competing financial interests or personal relationships that could have appeared to influence the work reported in this paper.

Acknowledgements

The authors would like to acknowledge the Fundação para a Ciência e Tecnologia (FCT) for funding the Ph.D. scholarship SFRH/BD/145037/2019 and the researcher position (UIDB/04708/2020 and

UIDP/04708/2020 - CONSTRUCT). This work was also financed through the Regional Operational Programme CENTRO2020 within the scope of the project CENTRO-01-0145-FEDER-000006, and the Fiber-Bridge – Fatigue strengthening and assessment of railway metallic bridges using fiber-reinforced polymers (POCI-01-0145-FEDER-030103) by FEDER funds through COMPETE2020 (POCI) and by national funds (PIDDAC) through the Portuguese Science Foundation (FCT/MCTES).

References

[1] Akesson B. Fatigue life of riveted steel bridges. 1st ed. CRC Press; 2010.
[2] Geissler K. Assessment of old steel bridges. Struct Eng Int 2002;12:258–63.
[3] Larsson T. Fatigue assessment of riveted bridges. PhD Thesis. Department of Civil and Environmental Engineering, Lulea University of Technology, 2009.
[4] Oehme P. Schäden an Stahltragwerken – eine Analyse (Damage Analysis of Steel Structures). IABSE Proc. P-139/89, 1989.
[5] Jorge R, Riberio A, De Jesus A, Figueiredo M, Castro M, Fernandes A. Ponte Eiffel - Viana do Castelo. Avaliação de Resultados de Programa Experimental (Eiffel bridge - Viana do Castelo. Experimental results evaluation). IDMEC/FEUP: Faculdade de Engenharia, Universidade Do Porto: 2006.
[6] Ghafoori E, Motavalli M. A retrofit theory to prevent fatigue crack initiation in aging riveted bridges using carbon fiber-reinforced polymer materials. Polymers (Basel) 2016;8:308.
[7] Ghafoori E, Prinz G, Mayor E, Nussbaumer A, Motavalli M, Herwig A, et al. Finite element analysis for fatigue damage reduction in metallic riveted bridges using pre-stressed CFRP plates. Polymers (Basel) 2014;6:1096–118.
[8] Ghafoori E, Motavalli M, Nussbaumer A, Herwig A, Prinz GS, Fontana M. Design criterion for fatigue strengthening of riveted beams in a 120-year-old railway metallic bridge using pre-stressed CFRP plates. Compos Part B Eng 2015;68:1–13.
[9] Ghafoori E, Hosseini A, Al-Mahaidi R, Zhao X-L, Motavalli M. Prestressed CFRP-strengthening and long-term wireless monitoring of an old roadway metallic bridge. Eng Struct 2018;176:585–605.
[10] ECCS. European Recommendations for Bolted Connections with Injection Bolts. 1st ed. Publication No 79; 1994.
[11] Correia J, Pedrosa B, Raposo P, Jesus A, Rebelo C, Gervásio H, et al. Fatigue strength evaluation of resin-injected bolted connections using statistical analysis. Engineering 2017;3(6):795–805.
[12] Hosseini S, Mamun M, Mirza O, Mashiri F. Behaviour of blind bolt shear connectors subjected to static and fatigue loading. Eng Struct 2020;214:110584.
[13] Qiu B, Yang X, Zhou Z, Lei H. Experimental study on fatigue performance of M30 high-strength bolts in bolted spherical joints of grid structures. Eng Struct 2020; 205:110123.
[14] Leonetti D, Maljaars J, Snijder H. Fatigue life prediction of hot-riveted shear connections using system reliability. Eng Struct 2019;186:471–83.
[15] Akyel A, Kolstein M, Bijlaard F. Fatigue strength of repaired welded connections made of very high strength steels. Eng Struct 2018;161:28–40.
[16] Liu N, Cui X, Xiao J, Lua J, Phan N. A simplified continuum damage mechanics based modeling strategy for cumulative fatigue damage assessment of metallic bolted joints. Int J Fatigue 2020;131:105302.
[17] Carpinteri A, Ronchei C, Scorza D, Vantadori S. Fracture mechanics based approach to fatigue analysis of welded joints. Eng Fail Anal 2015;49:67–78.
[18] Carpinteri A, Boaretto J, Fortese G, Giordani F, Iturrioz I, Ronchei C, et al. Fatigue life estimation of fillet-welded tubular T-joints subjected to multiaxial loading. Int J Fatigue 2017;101:263–70.
[19] CEN. EN 1090-2. Execution of steel structures and aluminium structures - Part 2: Technical requirements for steel structures. European Committee for Standardization; 2008.
[20] Gresnigt A, Sedlacek G, Paschen M. Injection Bolts To Repair Old Bridges. Http//CiteseerxIstPsuEdu/Viewdoc/Download?Doi=10115524959&rep=rep1&type=pdf (May 5, 2016) 2000:349–60.
[21] Mattes J. Substituição de Rebites por Parafusos Injectados com Resina (Replacement of Rivets by Resin Injection Bolts). MSc Thesis, IST. Portugal: University of Lisbon; 2007.
[22] Zafari B, Qureshi J, Mottram JT, Rusev R. Static and fatigue performance of resin injected bolts for a slip and fatigue resistant connection in FRP bridge engineering. Structures 2016;7:71–84.
[23] Rodrigues M, Correia J, Jesus A, Moreira P, Calçada R, Xavier J, et al. Static and fatigue behaviour of Sikadur®-30 and Sikadur®-52 structural resins/adhesives. International Conference on Structural Integrity, Portugal, 2017.
[24] Koper A. Assessment of Epoxy Resins for Injected Bolted Shear Connections. MSc Thesis. Delft University of Technology; 2017.
[25] Kolstein H, Li J, Koper A, Gard W, Nijgh M, Veljkovic M. Behaviour of double shear connections with injection bolts. Steel Constr 2017;10:287–94.
[26] Nijgh M. New materials for injected bolted connections - a feasibility study for demountable connections. MSc Thesis. Delft University of Technology; 2017.
[27] Xin H, Nijgh M, Veljkovic M. Computational homogenization simulation on steel reinforced resin used in the injected bolted connections. Compos Struct 2019;210: 942–57.
[28] Nijgh M, Xin H, Veljkovic M. Non-linear hybrid homogenization method for steel-reinforced resin. Constr Build Mater 2018;182:324–33.
[29] Kulak G, Fisher J, Struik J. Guide to design criteria for bolted and riveted joints. 2nd ed. Wiley-Interscience; 1987.
[30] Juoksukangas J, Lehtovaara A, Mäntylä A. Experimental and numerical investigation of fretting fatigue behavior in bolted joints. Tribol Int 2016;103: 440–8.
[31] Jiménez-Peña CH, Talemi R, Rossi B, Debruyne D. Investigations on the fretting fatigue failure mechanism of bolted joints in high strength steel subjected to different levels of pre-tension. Tribol Int 2017; 108: 128–40.
[32] Albrecht P, Sahli A, Wattar F. Fatigue strength of bolted joints. J Struct Eng 1987; 113:1834–49.
[33] Chakherlou T, Oskouei R, Vogwell J. Experimental and numerical investigation of the effect of clamping force on the fatigue behaviour of bolted plates. Eng Fail Anal 2008;15:563–74.
[34] Novoselac S, Kozak D, Ergić T, Damjanović D. Fatigue damage assessment of bolted joint under different preload forces and variable amplitude eccentric forces for high reliability BT - fracture at all scales. In: Pluvinage G, Milovic L, editors., Springer International Publishing; 2017, p. 239–68.
[35] Fernando U, Farrahi G, Brown M. Fretting fatigue crack growth behavior of BS L45 4 percent copper aluminium alloy under constant normal load. Fretting Fatigue ESIS 1994;18:183–95.
[36] Schijve J. Fatigue of Structures and Materials. New York: 2004.
[37] CEN. EN 1993-1-9: Eurocode 3, Design of steel structures – Part 1-9: Fatigue. Brussels: European Committee for Standardization; 2005.
[38] Russo F, Mertz D, Frank K, Wilson K. Design and Evaluation of Steel Bridges for Fatigue and Fracture – Reference Manual. Publication No. FHWA-NHI-16-016, Federal Highway Administration: 2016.
[39] Wang C, Wang Y, Duan L, Wang S, Zhai M. Fatigue performance evaluation and cold reinforcement for old steel bridges. Struct Eng Int 2019; 29: 563–9.
[40] Taras A, Greiner R. Development and application of a fatigue class catalogue for riveted bridge components. Struct Eng Int: J Int Assoc Bridge Struct Eng (IABSE), 2010; 20: 91–103.
[41] Di Battista J, Adamson D, Kulak G. Fatigue strength of riveted connections. J Struct Eng 1998.
[42] Jesus A, Silva A, Correia J. Fatigue of riveted and bolted joints made of puddle iron - An experimental approach. J Constr Steel Res 2015;104:81–90.
[43] Appleton J, Moura R. A utilização do aço inox na reabilitação das insfraestruturas da Ponte Eiffel sobre o Rio Lima , em Viana do Castelo Inspecção e Reabilitação (Rehabilitation of Eiffel bridge Infrastructures using stainless steel), ASCP'09 – 1°Congresso de Segurança e Conservação de Pontes ASCP - Lisbon: 2009, p. 3–10.
[44] Sika Portugal. Sikadur®-52. Product Data Sheet. Https://PrtSikaCom/Dms/GetdocumentGet/99182134-32ad-37e2-A2ca-33bc83235a54/76%20Sikadur%2052%20Injection_07608Pdf (June 19th, 2016) 2016.
[45] ISO/TC164/SC4. BS ISO 12107: Metallic materials — Fatigue testing — Statistical planning and analysis of data; 2012.
[46] Witkovsky V. ToleranceFactor (https://www.mathworks.com/matlabcentral/fileexchange/24135-tolerancefactor). MATLAB Cent File Exch 2021.
[47] Schneider C, Maddox S. Best practice guide on statistical analysis of fatigue data. Internation Institute of Welding, Doc IIW-XIII-WG1-114 - 03: 2003.
[48] CEN. Eurocode 3: Design of steel structures – Part 1-1: General rules and rules for buildings. Brussels: European Committee for Standardization; 2005.
[49] ASTM D7791 - 2012. Standard test method for uniaxial fatigue properties of plastics; 2012.
[50] Pedrosa B, Correia J, Rebelo C, Lesiuk G, De Jesus A, Fernandes A, et al. Fatigue resistance curves for single and double shear riveted joints from old portuguese metallic bridges. Eng Fail Anal 2019;96:255–73.